Preprints of the 21st IFAC World Congress (Virtual)
Berlin, Germany, July 12-17, 2020

Decentralized Formation Control for Multiple Quadrotors under Unidirectional Communication Constraints

Pedro Roque * **Shahab Heshmati-Alamdari** * **Alexandros Nikou** *
Dimos V. Dimarogonas *

* *KTH Royal Institute of Technology, Stockholm, Sweden*
{padr,shaha,anikou,dimos}@kth.se.

Abstract: This paper addresses the problem of formation control for multiple Unmanned Aerial Vehicles (UAVs) with relative sensing capabilities and operating under input–state limitations. More specifically, we propose a novel distributed leader-follower architecture for a team of aerial robots to follow cooperatively a desired path while maintaining a predefined formation geometry. In the proposed control strategy, knowledge of the desired formation path is restricted to the leader UAV, which can also broadcast its state information to all followers. In this way, the leader UAV, by employing a Nonlinear Model Predictive Control (NMPC) law, tries to navigate the whole group of agents towards the desired path while ensuring the connectivity of the team. More specifically, in order to maintain the connectivity, the leading UAV estimates the followers motion, by employing a fast geometric propagation that exploits the knowledge of the desired formation and sensing capabilities. On the other hand, the followers estimate the motion of the leading UAV by receiving its local state information and implementing a NMPC law that achieves tracking of the desired formation and maintains the connectivity with respect to the leader UAV.

1. INTRODUCTION

During the last decades, considerable progress has been made in the field of Unmanned Aerial Vehicles (UAVs), with a significant number of results in a variety of aerial surveillance activities, as in Tsourdos et al. (2010).

Classic approaches such as feedback linearization in Akhtar et al. (2012), Lyapunov based stabilization in Castillo et al. (2004), dynamic inversion in Das et al. (2009), PID and LQR in Tayebi and McGilvray (2006) and backstepping in Frazzoli et al. (2000) have been used in the past to design motion controllers for rotary wing aerial robots. Nevertheless, the aforementioned methods yield poor closed-loop performance and the results were local, around only selected operating points. In addition, the aforementioned motion control strategies do not guarantee input and state constraints. In this context, Nonlinear Model Predictive Control (NMPC) Allgöwer et al. (2004) is a suitable approach for complex surveillance missions, as it is able to combine motion planning with input and state constraints satisfaction, as in Heshmati-Alamdari et al. (2019).

Most of the aerial surveillance tasks can be carried out more efficiently if multiple UAVs are cooperatively involved, as shown in Chen et al. (2010). Therefore, cooperation between multiple UAVs, and especially the decentralized case, gained a significant attention during the last years. Decentralized cooperative schemes usually depend on explicit communication among the robots (e.g., online sharing of all internal and external information to improve coordination performance, as in Rucco et al. (2015)). For instance, in Bemporad and Rocchi (2011) decentralized control strategies have been proposed for formation of UAVs considering obstacles and collision avoidance constraints. However, employing all of the aforementioned strategies requires each robot to communicate with the whole team. This requires an accurate common global localization system for all participating robots which is either difficult to be achieved in indoor environments or in the most optimistic case would raise the mission cost. Moreover, in general, such approaches may become infeasible, in terms of bandwidth and computational complexity, as shown in Rucco et al. (2015).

Motivated by the aforementioned considerations, this work presents a novel cooperative control framework for a group of multiple UAVs in order to follow a desired path while maintaining a predefined formation geometry and satisfying input and state constraints. In particular, we propose a novel decentralized leader-follower architecture, where the leader UAV, which has knowledge over a predefined formation geometry and desired path, tries to navigate the whole group of agents while ensuring the connectivity of the team. More specifically, in order to maintain the connectivity, the leader UAV estimates the followers' motion, by employing a fast geometric propagation that exploits the knowledge of the desired formation and sensing capabilities. On the other hand, the followers estimate the motion of the leader UAV, by receiving its local state information and implementing a NMPC law that tracks the desired formation and maintains the connectivity with respect to the leader UAV. Specifically, no explicit data is sent from the followers to other agents involved in the cooperative task, making in this way the whole system scalable regarding the number of agents involved in it.

⋆ This work was supported by the H2020 ERC Grant BUCOPHSYS, the EU H2020 Co4Robots project, the Swedish Foundation for Strategic Research (SSF), the Swedish Research Council (VR) and the Knut och Alice Wallenberg Foundation (KAW).

Copyright lies with the authors

2. PROBLEM FORMULATION

Consider $M+1$ aerial robotic agents under a single leader - multiple followers architecture operating in a workspace $\mathcal{W} \subset \mathbb{R}^3$. We denote the agents state vectors by $\boldsymbol{\xi}_i$, $i \in \mathcal{A} = \{L, F_1, \ldots, F_M\}$, where L represents the leader, $F_1 \ldots F_M$ the followers. Let $\mathcal{F} = \mathcal{A} \backslash L$. More precisely, $\boldsymbol{\xi}_i \triangleq [\mathbf{x}_i, \mathbf{v}_i, \mathbf{q}_i, \boldsymbol{\omega}_i]^T \in \mathbb{R}^3 \times \mathbb{R}^3 \times \mathbb{S}^3 \times \mathbb{R}^3$, $i \in \mathcal{A}$, includes the position (i.e., $\mathbf{x}_i = [x_i,\ y_i,\ z_i]^\top \in \mathbb{R}^3$), linear velocity (i.e., $\mathbf{v}_i = [u_i,\ v_i,\ w_i]^\top \in \mathbb{R}^3$), attitude quaternion (i.e., $\mathbf{q}_i \in \mathbb{S}^3$), and angular velocity ($\boldsymbol{\omega}_i \in \mathbb{R}^3$) vectors for agent i. Unless otherwise stated, $\mathbf{x}_i$ and $\mathbf{v}_i$ are represented in the inertial frame $\mathfrak{I}$, while $\mathbf{q}_i$ and $\boldsymbol{\omega}_i$ are represented in the body frame of agent i. Relative positions in the agents' body frame are defined as $\boldsymbol{\chi}_{ij}$, and represent the position of agent j, in the frame of agent i. It is often more practical to use rotation matrices that are derived from the attitude quaternion $\mathbf{q}$. Such matrices are represented as $\mathbf{R}_{\mathsf{i}/\mathsf{b}}(\mathbf{q}_i) : \mathbb{S}^3 \rightarrow \mathbb{SO}(3)$ and rotate a vector from frame i to frame b. When the target frame is the inertial frame $\mathfrak{I}$, then this frame might be omitted, as in $\mathbf{R}_{\mathsf{i}/\mathfrak{I}} = \mathbf{R}_{\mathsf{i}}$. Accordingly, all rotation matrices $\mathbf{R}_{\mathsf{i}/\mathfrak{I}}$ have the property $||\mathbf{R}_{\mathsf{i}/\mathfrak{I}}|| = 1$ and $\det(\mathbf{R}_{\mathsf{i}/\mathfrak{I}}) = 1$. Without loss of generality, according to the standard aerial vehicle's modeling properties in Mahony et al. (2012), the dynamic equations of each agent $i \in \mathcal{A}$ can be given as:

$$\dot{\mathbf{x}}_i = \mathbf{v}_i, \;\; \dot{\mathbf{v}}_i = \mathbf{R}_{\mathsf{i}} \frac{\boldsymbol{\nu}_i}{m_i} + \mathbf{g}, \tag{1a}$$

$$\dot{\mathbf{q}}_i = \frac{1}{2}\Omega(\mathbf{q}_i)\boldsymbol{\omega}_i, \;\; \dot{\boldsymbol{\omega}}_i = \mathbf{J}_i^{-1}(\boldsymbol{\tau}_i - \boldsymbol{\omega}_i \times \mathbf{J}_i\boldsymbol{\omega}_i), \tag{1b}$$

where m_i is the vehicle's mass, $\mathbf{g}$ the gravity vector expressed in the inertial frame $\mathfrak{I}$, $\mathbf{J}_i$ the vehicle's inertia matrix, $\boldsymbol{\tau}_i \in \mathbb{R}^3$ is the 3-DoF (Degree-of-Freedom) torque vector in the body frame, and $\Omega(\mathbf{q}_i)$ is defined as:

$$\Omega(\mathbf{q}_i) = \begin{bmatrix} q_{i(w)} & -q_{i(z)} & q_{i(y)} \\ q_{i(z)} & q_{i(w)} & -q_{i(x)} \\ -q_{i(y)} & q_{i(x)} & q_{i(w)} \\ -q_{i(x)} & -q_{i(y)} & -q_{i(z)} \end{bmatrix}$$

Moreover, $\boldsymbol{\nu}_i \triangleq [0\ \ 0\ \ \nu_{i(z)}]^T$ represents a 1-DoF thrust aligned with the z axis of the agent body frame. From now on, we denote by $\mathbf{u}_i \triangleq \left[\nu_{i(z)}, \boldsymbol{\tau}_i^T\right]^T \in \mathbb{R}^4$ the concatenated control input of the robotic agent i. Based on the aforementioned considerations, the dynamics of (1a)-(1b), can be written in discrete-time form as:

$$\boldsymbol{\xi}_i(k+n+1|k) = f_i(\boldsymbol{\xi}_i(k+n|k), \mathbf{u}_i(k+n|k)),\ i \in \mathcal{A}, \tag{2}$$

where $f_i : \mathbb{R}^9 \times \mathbb{S}^3 \times \mathbb{R}^4 \rightarrow \mathbb{R}^9 \times \mathbb{S}^3$ defines the discrete-time dynamics for (1a)-(1b), discretized through a zero-order-hold (ZOH) sampling method. We denote estimations for time $k+n$ at time k as $(k+n|k)$ and measurements at time k as (k). Assume that the velocity that the UAV can generate is bounded by $v_{i_{Max}}$, $i \in \mathcal{A}$. Moreover, quaternions are unit-norm vectors. These requirements are captured by the state constraint set Ξ_i, given by

$$\Xi_i \triangleq \{\boldsymbol{\xi}_i \in \mathbb{R}^9 \times \mathbb{S}^3 : ||\mathbf{v}_i|| \leq v_{i_{Max}}, ||\mathbf{q}_i|| = 1\},\ i \in \mathcal{A}. \tag{3}$$

The actuation forces and torques are generated by the thrusters. Thus, we define the control constraint set U_i, $i \in \mathcal{A}$, corresponding to the physical actuator limits, as follows:

$$U_i \triangleq \Big\{\mathbf{u}_i \in \mathbb{R}^4 : -\tfrac{\nu_{i_{(z)}}}{4} a_{l_i} \leq \tau_{(x,y)} \leq \tfrac{\nu_{i_{(z)}}}{4} a_{l_i}, \\ -0.01 \leq \tau_{(z)} \leq 0.01, 0 \leq \nu_{i_{(z)}} \leq 4 \cdot 9.81 \cdot m_i\Big\}, \tag{4}$$

where a_{l_i} is the quadrotor's arm length, i.e., the distance between the center of the UAV and the motors.

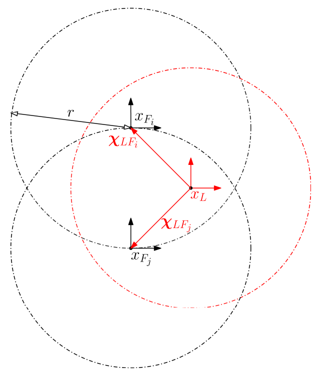

Fig. 1. Connectivity for a team of agents including one leader and two followers. The sensing areas are denoted by $\mathcal{B}(\mathbf{x}_i, r)$, $i \in \mathcal{A}$.

Consider the set of agents $\mathcal{A} = \{L, F_1 \ldots, F_M\}$. Without loss of generality, let $\mathcal{B}(\mathbf{x}_i, r)$ be a sensing area where the agent $i \in \mathcal{A}$ can measure a relative distance d_{ij} and a unitary relative bearing vector $\boldsymbol{\beta}_{ij}$ with respect to its neighbor $j \in \mathcal{N}_i$, where

$$\mathcal{N}_i \triangleq \{j \in \mathcal{A}, j \neq i : ||\mathbf{x}_i - \mathbf{x}_j|| \leq r\}. \tag{5}$$

It should be noted that $\mathcal{N}_i$ denotes the agents that are required to remain connected (see Fig 1). The aforementioned values can be defined as

$$d_{ij} = ||\mathbf{x}_j - \mathbf{x}_i||,\ \ \boldsymbol{\beta}_{ij} = \mathbf{R}_{\mathsf{i}}^T \frac{\mathbf{x}_j - \mathbf{x}_i}{d_{ij}},\ \ \boldsymbol{\chi}_{ij} = d_{ij}\, \boldsymbol{\beta}_{ij}, \tag{6}$$

where $d_{ij} > 0$. Note that from a range d_{ij} and bearing $\boldsymbol{\beta}_{ij}$ we can uniquely reconstruct $\boldsymbol{\chi}_{ij}$ - the relative position of agent j in the frame of i - and that these measurements can be obtained locally, therefore requiring no communication. Accordingly, the formation geometry is defined as

$$\hat{\boldsymbol{\chi}}_{ij} = \hat{d}_{ij}\, \hat{\boldsymbol{\beta}}_{ij},\ i \in \mathcal{F}, j \in \mathcal{N}_i, \tag{7}$$

where $\hat{d}_{ij}$, $\hat{\boldsymbol{\beta}}_{ij}$ and $\hat{\boldsymbol{\chi}}_{ij}$ are desired relative distances, bearings and positions. Note that each follower $i \in \mathcal{F}$ is only aware of it own desired relative distance, bearing and position with respect to the leader UAV.

Moreover, we consider that each follower i, $i \in \mathcal{F}$ receives a set of information broadcasted by the leader denoted as

$$\mathbf{w}_L = [\boldsymbol{\xi}_L^T, \hat{\mathbf{v}}_L^T]^T \in \mathbb{R}^{12} \times \mathbb{S}^3 \subset W \tag{8}$$

where $\hat{\mathbf{v}}_L$ is the reference leader velocity on the desired path Akhtar et al. (2012); Gandolfo et al. (2016) and W is a compact set capturing the information broadcasted by the leader and satisfies $W \subset \Xi_L$.

Problem 1. Consider $M+1$ UAVs described by (2), with state and input constraints imposed by the sets Ξ_i, U_i, $i \in \mathcal{A}$, given in (3) and (4), respectively. Considering that i) only the leader UAV is aware of a desired path, and ii) the followers have access only to information broadcasted by the leader UAV defined in (8), design a distributed control protocol $\boldsymbol{u}_i$, $i \in \mathcal{A}$, that impose the team of agents to follow cooperatively the desired path $\boldsymbol{p}_d$ while guaranteeing i) the maintenance of the predefined formation geometry in (7), and ii) the connectivity among the agents with respect to their sensing capabilities defined in (5).

3. CONTROL METHODOLOGY

We propose a control strategy that requires the desired path $\boldsymbol{p}_d$ to be known and tracked by the leader. The leader UAV navigates the whole team by keeping the whole group connected and organized according to the desired relative positions (7). We propose a Decentralized Nonlinear Model Predictive Control-based (DNMPC) approach to solve Problem 1.

3.1 Control Strategy

At each sample time k, a cost function $\boldsymbol{J}_i(\cdot)$, $i \in \mathcal{A}$, is minimized with respect to a control sequence $\mathbf{u}_i = \{\mathbf{u}_i(k|k), \mathbf{u}_i(k+1|k), \dots, \mathbf{u}_i(k+N-1|k)\}$, yielding N predicted states $\{\boldsymbol{\xi}_i(k+1|k), \dots, \boldsymbol{\xi}_i(k+N|k)\}$ by applying the optimal control input to the agents dynamics. We also have that $\boldsymbol{\xi}_i(k|k) = \boldsymbol{\xi}_i(k)$, corresponding to the actual feedback of agent i at time k. Depending on the agent's role - either leader or follower - different assumptions and costs $\boldsymbol{J}_i(\cdot)$ are defined.

Error Definition The vector of errors for the leader UAV as well as followers UAVs are, respectively,

$$\mathbf{e}_L = \begin{bmatrix} \mathbf{e}_{LF} \\ \mathbf{e}_{v_L} \\ e_{\mathbf{R}_L} \end{bmatrix} = \begin{bmatrix} \sum_{F_i \in \mathcal{N}_L} (\hat{\boldsymbol{\chi}}_{LF_i} - \boldsymbol{\chi}_{LF_i}) \\ \hat{\mathbf{v}}_L - \mathbf{v}_L \\ e_{\mathbf{R}_L}(\mathbf{R}_L, \hat{\mathbf{R}}_L) \end{bmatrix} \in \mathbb{R}^7, \tag{9a}$$

$$\mathbf{e}_{F_i} = \begin{bmatrix} \mathbf{e}_{F_i L} \\ \mathbf{e}_{vF_i} \\ e_{\mathbf{R}_i} \end{bmatrix} = \begin{bmatrix} \hat{\boldsymbol{\chi}}_{F_i L} - \boldsymbol{\chi}_{F_i L} \\ \hat{\mathbf{v}}_{F_i} - \mathbf{v}_{F_i} \\ e_{\mathbf{R}_{F_i}}(\mathbf{R}_{F_i}, \hat{\mathbf{R}}_{F_i}) \end{bmatrix} \in \mathbb{R}^7,\ i \in \mathcal{F}, \tag{9b}$$

where $\hat{\mathbf{v}}_{F_i}$ is the reference leader velocity (i.e., $\hat{\mathbf{v}}_L$ broadcasted by the leader) transformed to the followers body frame, $\hat{\mathbf{R}}_i,\ i \in \mathcal{A}$, is a predefined desired attitude for the agents in the formation, and $e_{\mathbf{R}_i}(\mathbf{R}_i, \hat{\mathbf{R}}_i)$ the same as of eq. (8) in Lee et al. (2010), $e_{\mathbf{R}_i}(\mathbf{R}_i, \hat{\mathbf{R}}_i) = \frac{1}{2} tr(\mathbf{I} - \hat{\mathbf{R}}_i^T \mathbf{R}_i)$, where $tr(\cdot)$ is the trace operator. Note that $e_{\mathbf{R}_i}(\mathbf{R}_i, \hat{\mathbf{R}}_i) \in [0, 2)$. The feasible error sets are defined as:

$$E_L = \{\mathbf{e}_L \in \mathbb{R}^7 : \{\{\hat{\boldsymbol{\chi}}_{L_i}\} \ominus \Xi_{F_i} \ominus \Xi_L\} \cup \{\{\hat{\mathbf{v}}_L\} \ominus \{\mathbf{v}_L\}\} \cup [0, 2)\} \tag{10a}$$

$$E_{F_i} = \{\mathbf{e}_{F_i} \in \mathbb{R}^7 : \{\{\hat{\boldsymbol{\chi}}_{F_i L}\} \ominus \Xi_L \ominus \Xi_{F_i}\} \cup \{\{\mathbf{v}_{F_i}\} \ominus \{\hat{\mathbf{v}}_{F_i}\}\} \cup [0, 2)\} \tag{10b}$$

3.2 Leader Control Framework

The following section defines the controller for the formation leader, as well as the propagation method used to predict the followers motion. We assume that the leader has access to its state $\boldsymbol{\xi}_L$, relative distance d_{LF_i} and bearing $\boldsymbol{\beta}_{LF_i}$ measurements, with corresponding desired values $\hat{d}_{LF_i}$ and $\hat{\boldsymbol{\beta}}_{LF_i}$, for all $i \in \mathcal{N}_i$, given in (7). Note that $d_{LF_i} = d_{F_i L}$, but $\boldsymbol{\beta}_{LF_i} \neq \boldsymbol{\beta}_{F_i L}$, due to (6), which results in $\boldsymbol{\chi}_{LF_i} \neq \boldsymbol{\chi}_{F_i L}$. We further consider a prediction function $\Upsilon_{e_i}(\cdot)$, which will be defined hereafter, predicting the relative position of the followers for a time horizon $k + n,\ n = 1, \dots, N$, based only on the measurements $\boldsymbol{\chi}_{LF_i}(k) = d_{LF_i} \boldsymbol{\beta}_{LF_i}$ obtained at time k.

Now we are ready to formulate the NMPC problem for the leading agent L as

$$\begin{aligned} \min_{\mathbf{u}_L} J_L = \min_{\mathbf{u}_L} \sum_{n=0}^{N-1} \big[& \boldsymbol{J}_P\big(\mathbf{e}_{v_L}(k+n|k), \mathbf{u}_L(k+n|k)\big) + \\ & \boldsymbol{J}_Q\big(\mathbf{e}_{LF}(k+n|k)\big) + \boldsymbol{J}_A\big(e_{\mathbf{R}_L}(k+n|k)\big)\big] + \\ & \boldsymbol{J}_V\big(\mathbf{e}_{v_L}(k+N|k)\big). \end{aligned} \tag{11}$$

subject to

$$\begin{aligned} & \xi_L(k+n+1|k) = f_L\big(\xi_L(k+n|k), \mathbf{u}_L(k+n|k)\big) \\ & \mathbf{e}_{LF}(k+n+1|k) = \sum_{F_i \in \mathcal{N}_L} \Upsilon_{e_{F_i}}\Big(\hat{\boldsymbol{\chi}}_{LF_i} - \boldsymbol{\chi}_{LF_i}(k+n|k), v_{i_{\mathsf{Max}}}\Big) \\ & \quad \mathbf{e}_L(k+n|k) \in E_L,\ \ \mathbf{e}_L(k+N|k) \in E_L^f \\ & \quad \mathbf{u}_L(k+n|k) \in U_L\ \ , n = 0, \dots, N-1, \end{aligned}$$

where

$$\boldsymbol{J}_P\big(\mathbf{e}_{v_L}(k+n|k), \mathbf{u}_L(k+n|k)\big) = \\ = \|\mathbf{e}_L(k+n|k)\|_{Q_V} + \|\mathbf{u}_L(k+n|k)\|_{Q_R}, \tag{12a}$$

$$\boldsymbol{J}_Q\big(\mathbf{e}_{LF}(k+n|k)\big) = \|\mathbf{e}_{LF}(k+n|k)\|_{Q_F}, \tag{12b}$$

$$\boldsymbol{J}_A\big(e_{\mathbf{R}_L}(k+n|k)\big) = \|e_{\mathbf{R}_L}(k+n|k)\|_{Q_A} \tag{12c}$$

$$\boldsymbol{J}_V\big(\mathbf{e}_{v_L}(k+N|k)\big) = \|\mathbf{e}_{v_L}(k+N|k)\|_{Q_N}, \tag{12d}$$

and where $E_L^f \subset E_L$ is the terminal set, $v_{i_{\mathsf{Max}}}$ the maximum velocity for all $i \in \mathcal{N}_i$ given in (3), and Q_F, Q_V, Q_R, Q_A and Q_N are positive definite diagonal weighing matrices (Q_A is a scalar).

Follower Position Propagation Let $\boldsymbol{\chi}_{LF_i}(k)$ be the relative position of agent i in the frame of the formation leader, at time k. This position is calculated based on the leader measurements i.e, $d_{LF_i}(k)$ and $\boldsymbol{\beta}_{LF_i}(k)$ through equation (6).

Taking into account the state constraints in (3), a ball $\mathcal{B}(\boldsymbol{\chi}_{LF_i}(k+n|k), \Delta v_{i_{\mathsf{Max}}}\delta)$ defines the set of all possible relative positions $\boldsymbol{\chi}_{LF_i}(k+n+1|k)$ where $\Delta v_{i_{\mathsf{Max}}} = v_{i_{\mathsf{Max}}} - \|\mathbf{v}_L(k+n|k)\|$, and δ is a constant sampling interval; $\mathcal{B}(\boldsymbol{\chi}_{LF_i}(k), \Delta v_{i_{\mathsf{Max}}}\delta)$ represents the set of all possible positions for the neighbor i over one step of the controller.

The formation leader, acting as a central coordinator in the formation setting, assumes that the followers strive to achieve their desired positions as fast as possible, navigating at maximum velocity to do so. However, as the movement is relative to the leader, its velocity also influences the set of possible positions to be achieved by the followers. The relative position propagation of the followers in the leader frame through the whole receding horizon is then

$$\begin{aligned} \Upsilon_{F_i}(\boldsymbol{\chi}_{LF_i}(k+n|k), \hat{\boldsymbol{\chi}}_{LF_i}, v_{i_{\mathsf{Max}}}) &= \boldsymbol{\chi}_{LF_i}(k+n|k) + \\ &+ \frac{\hat{\boldsymbol{\chi}}_{LF_i} - \boldsymbol{\chi}_{LF_i}(k+n|k)}{\|\hat{\boldsymbol{\chi}}_{LF_i} - \boldsymbol{\chi}_{LF_i}(k+n|k)\|}(v_{i_{\mathsf{Max}}} - \|\mathbf{v}_L\|) \cdot \\ &\cdot (1 - e^{-\alpha \cdot \|\hat{\boldsymbol{\chi}}_{LF_i} - \boldsymbol{\chi}_{LF_i}(k+n|k)\|}) \cdot \delta, \end{aligned} \tag{13}$$

where α is a tuning parameter that adjusts the speed gradient of the followers prediction, and e^x the exponential of x.

Finally, it is convenient to define the function Υ_i in terms of the error $\mathbf{e}_{LF}$, so that we can include it on the NMPC formulation:

$$\mathbf{e}_{LF}(k+n|k) = \sum_{F_i \in \mathcal{N}_L} \big(\hat{\boldsymbol{\chi}}_{LF_i} - \boldsymbol{\chi}_{LF_i}(k+n|k)\big) \tag{14}$$

$$\begin{aligned} \mathbf{e}_{LF}(k+n+1|k) &= \\ &= \sum_{F_i \in \mathcal{N}_L} \hat{\boldsymbol{\chi}}_{LF_i} - \Upsilon_{F_i}(\boldsymbol{\chi}_{LF_i}(k+n|k), \hat{\boldsymbol{\chi}}_{LF_i}, v_{i_{\mathsf{Max}}}) = \\ &= \sum_{F_i \in \mathcal{N}_L} \Upsilon_{e_{F_i}}(\boldsymbol{\chi}_{LF_i}(k+n|k), \hat{\boldsymbol{\chi}}_{LF_i}, v_{i_{\mathsf{Max}}}). \end{aligned} \tag{15}$$

3.3 Followers Control Framework

The follower's objective is to maintain a desired relative position with respect to the leader. The followers $i \in \mathcal{N}_L$ do not possess any knowledge over the desired formation path, which is known only to the formation leader. The leader, then, broadcasts through $\mathbf{w}_L(k)$ the velocity that it tracks at time k, which the followers use to unify the formation movement. This means that the desired tracking velocity is kept constant for all followers along the receding horizon, whereas the leader can update this desired velocity based on its predicted states. Accordingly, we assume that the followers have access to their state $\boldsymbol{\xi}_{F_i}$, the relative distance d_{F_iL} and bearing $\boldsymbol{\beta}_{F_iL}$ measurements, as well as to the desired formation constraints - $\hat{d}_{F_iL}$ and $\hat{\boldsymbol{\beta}}_{F_iL}$. We are ready to define the NMPC for the followers as:

$$\min_{\mathbf{u}_{F_i}} J_{F_i} = \min_{\mathbf{u}_{F_i}} \sum_{n=0}^{N-1} \big[\boldsymbol{J}_P\big(\mathbf{e}_{v_{F_i}}(k+n|k), \mathbf{u}_{F_i}(k+n|k)\big)+ \\ + \boldsymbol{J}_Q\big(\mathbf{e}_{F_iL}(k+n|k), \mathbf{w}_L(k)\big) + \boldsymbol{J}_A\big(e_{\mathbf{R}_{F_i}}(k+n|k)\big)\big]+ \\ + \boldsymbol{J}_V\big(\mathbf{e}_{v_{F_i}}(k+N|k)\big). \tag{16}$$

subject to

$$\xi_{F_i}(k+n+1|k) = f_{F_i}\big(\xi_{F_i}(k+n|k), \mathbf{u}_{F_i}(k+n|k)\big)$$
$$\mathbf{e}_{F_iL}(k+n+1|k) = g_{e_L}\big(\mathbf{e}_{F_iL}(k+n|k), \mathbf{w}_L(k)\big)$$
$$\mathbf{e}_{F_i}(k+n|k) \in E_{F_i}, \mathbf{u}_{F_i}(k+n|k) \in U_{F_i} \ , n = 0, \ldots, N-1$$
$$\mathbf{e}_{F_i}(k+N|k) \in E_{F_i}^f, \ \ \mathbf{w}_L(k) \in W$$

where

$$\boldsymbol{J}_P\big(\mathbf{e}_{v_{F_i}}(k+n|k), \mathbf{u}_{F_i}(k+n|k)\big) = \\ = \|\mathbf{e}_{v_{F_i}}(k+n|k)\|_{Q_V} + \|\mathbf{u}_{F_i}(k+n|k)\|_{Q_R}, \tag{17a}$$
$$\boldsymbol{J}_Q\big(\mathbf{e}_{F_iL}(k+n|k)\big) = \|\mathbf{e}_{F_iL}(k+n|k)\|_{Q_F}, \tag{17b}$$
$$\boldsymbol{J}_A\big(e_{\mathbf{R}_{F_i}}(k+n|k)\big) = \|e_{\mathbf{R}_i}(k+n|k)\|_{Q_A} \tag{17c}$$
$$\boldsymbol{J}_V\big(\mathbf{e}_{v_{F_i}}(k+N|k)\big) = \|\mathbf{e}_{v_{F_i}}(k+N|k)\|_{Q_N}, \tag{17d}$$

and where $E_{F_i}^f \subset E_{F_i}$ is the terminal set and Q_A, Q_F, Q_V, Q_R and Q_N are positive definite diagonal weighing matrices - Q_A is again a scalar matrix. Moreover, $g_{e_L}\big(\mathbf{e}_{F_iL}(k+n|k), \mathbf{w}_L(k)\big)$ is a propagation process used for prediction of the relative error with respect to the leader UAV (i.e., $\mathbf{e}_{F_iL}(k+n+1|k)$), defined hereafter.

Leader Position Propagation: In order to estimate the relative position of the leader along a horizon of length N, the followers measure d_{F_iL} and $\boldsymbol{\beta}_{F_iL}$ at the sampled instant k which, from (6), uniquely define $\boldsymbol{\chi}_{F_iL}(k)$, $i \in \mathcal{F}$. Having the vector of $\mathbf{w}_L(k)$ broadcasted from the leader to all followers, the prediction for the leader position over the receding horizon, on behalf of follower i, for $n = 0, \ldots, N-1$ is given as:

$$\boldsymbol{\chi}_{F_iL}(k+n+1|k) = g_L\big(\boldsymbol{\chi}_{F_iL}(k+n|k), \mathbf{w}_L(k)\big) \\ = \boldsymbol{\chi}_{F_iL}(k+n|k) + \mathbf{R}_{F_i}^T(k+n|k)\,[\mathbf{v}_L(k) - \mathbf{v}_{F_i}(k+n)]. \tag{18}$$

With (9b), the dynamics (18) in error form can be rewritten

$$\mathbf{e}_{F_iL}(k+n+1|k) = g_{e_L}\big(\mathbf{e}_{F_iL}(k+n|k), \mathbf{w}_L(k)\big) \\ = \hat{\boldsymbol{\chi}}_{F_iL} - \boldsymbol{\chi}_{F_iL}(k+n|k) - \mathbf{R}_{F_i}^T(k+n|k)\,[\mathbf{v}_L(k) - \mathbf{v}_{F_i}(k+n)] \\ = \mathbf{e}_{F_iL}(k+n|k) - \mathbf{R}_{F_i}^T(k+n|k)\,[\mathbf{v}_L(k) - \mathbf{v}_{F_i}(k+n)].$$

4. STABILITY ANALYSIS

Before proceeding to the necessary analysis of the proposed NMPC strategy, we employ standard stability conditions that are used in MPC frameworks:

Assumption 1. Consider the running costs $J_{l_i}(\mathbf{e}_i, \mathbf{u}_i) = J_{Q_i}(\mathbf{e}_i) + \boldsymbol{J}_P\big(\mathbf{e}_i, \mathbf{u}_i\big)$, and the terminal cost function $\boldsymbol{J}_V(\mathbf{e}_i)$ for the formation leader, such that:

(1) E_L, E_L^f, and U_L are closed sets containing the origin, and E_L^f is a control invariant terminal set containing the origin;
(2) The cost functions $J_\star(\mathbf{e}(\cdot))$, as well as system dynamics and propagation functions f_e and Υ_{e_i}, are Lipschitz continuous, with Lipschitz constants $L_{J_\star}$, where $\star = \{P, Q, V\}$;

Property 1. In view of (9a), the difference between the nominal prediction state-error and the real state-error of the relative position of the followers relative to the leader is defined as $\|\mathbf{e}_{LF}(k+n|k) - \mathbf{e}_{LF}(k+n)\| = \sum_{F_i \in \mathcal{N}_L} \|\boldsymbol{\chi}_{LF_i}(k+n|k) - \boldsymbol{\chi}_{LF_i}(k+n)\| \leq \sum_{F_i \in \mathcal{N}_L} \Delta v_{i_{Max}} \delta_t \cdot n.$

Regarding the followers, their prediction of the leader movement is based on the information vector $\mathbf{w}_L(k)$. We have:

Lemma 1. The difference between the actual state $\mathbf{e}_{F_iL}(k+n)$ at time $k+n$ and the predicted state $\mathbf{e}_{F_iL}(k+n|k)$ at the same time under the control law defined in (16), is upper bounded by: $\|\mathbf{e}_{F_iL}(k+n|k) - \mathbf{e}_{F_iL}(k+n)\| \leq (1+L_f^n)\|\mathbf{x}_L(k) - \mathbf{x}_{F_i}(k)\| + (1+n)v_{L_{Max}} + \Big(\sum_{n=0}^N L_f^n\Big) L_u \|\mathbf{u}_L(k) - \mathbf{u}_{F_i}(k)\|.$

Proof. Initially notice that $\mathbf{e}_{F_{iL}}(k+1|k) = \hat{\boldsymbol{\chi}}_{F_{iL}} - \boldsymbol{\chi}_{F_{iL}}(k) - \mathbf{R}_{F_i}^T(k)\,[\mathbf{v}_L(k) - \mathbf{v}_{F_i}(k)]$ and $\mathbf{e}_{F_{iL}}(k+1) = \hat{\boldsymbol{\chi}}_{F_iL} - \boldsymbol{\chi}(k+1) = \hat{\boldsymbol{\chi}}_{F_{iL}} - \mathbf{R}_{F_i}^T(k+1)\,[\mathbf{x}_L(k+1) - \mathbf{x}_{F_i}(k+1)]$. From the equations, at step $n = 1, ..., N$, and the fact that $||\mathbf{R}_{F_i}^T(k)|| = 1, \forall k \in \mathbb{N}$ we get the general form

$$||\mathbf{e}_{F_iL}(k+n|k) - \mathbf{e}_{F_iL}(k+n)|| = \\ = || - \mathbf{R}_{F_i}^T(k)[\mathbf{x}_L(k) - \mathbf{x}_{F_i}(k)] - \\ [n+1]\mathbf{R}_{F_i}^T(k)\,[\mathbf{v}_L(k) - \mathbf{v}_{F_i}(k+n)] + \\ + \mathbf{R}_{F_i}^T(k+n)[\mathbf{x}_L(k+n) - \mathbf{x}_{F_i}(k+n)]|| \\ \leq ||\mathbf{x}_L(k) - \mathbf{x}_{F_i}(k)|| + (n+1)\cdot 2v_{L_{Max}} + \\ + ||\mathbf{x}_L(k+n) - \mathbf{x}_{F_i}(k+n)|| \leq \\ \leq (1+L_f^n)||\mathbf{x}_L(k) - \mathbf{x}_{F_i}(k)|| + (n+1)\cdot 2v_{L_{Max}} + \\ + \Big(\sum_{n=0}^N L_f^n\Big) L_u \|\mathbf{u}_L(k) - \mathbf{u}_{F_i}(k)\| = \gamma + \rho + \kappa,$$

where $\gamma = (1+L_f^n)\|\mathbf{x}_L(k) - \mathbf{x}_{F_i}(k)\|$, $\rho = (n+1)\cdot 2v_{L_{Max}}$, and $\kappa = \Big(\sum_{n=0}^N L_f^n\Big) L_u \|\mathbf{u}_L(k) - \mathbf{u}_{F_i}(k)\|$.

We are now ready to state the result of this work:

Theorem 1. Consider the team of UAVs described by (2), which are subject to constraints (3) and (4). The control inputs provided by (11), (12a)-(12d) as well as (16), (17a)-(17d) drive the errors $\boldsymbol{e}_L$ and $\boldsymbol{e}_{F_i}$, $i \in \mathcal{F}$, to sets E_L^f and $E_{F_i}^f$, $i \in \mathcal{F}$, containing the origin, while satisfying the constraints imposed by the sets E_i, U_i, $i \in \mathcal{A}$, given in (10a)-(10b) and (4) respectively.

Proof. Let us define $\mathcal{B}_L^n = \{\mathbf{z} : ||\mathbf{z}|| \leq \Delta v_{i_{Max}} \delta_t \cdot n\}, \forall n = 0 \ldots N$, and $\mathcal{B}_{F_i}^n = \{\mathbf{z} : ||\mathbf{z}|| \leq \gamma + \rho + \kappa\}, \forall n = 0, 1, \ldots, N$. By restricting the constraints over the horizon as $E_L \ominus \mathcal{B}_L^n$, $E_{F_i} \ominus \mathcal{B}_{F_i}^n$, and employing similar arguments to (Marruedo et al., 2002, Theorem 1, page. 4), we conclude that for every $n = 0, 1, \ldots, N$ it holds that $\mathbf{u}_{F_i}(k+n|k) \in \mathbb{U}_{F_i}$, $\mathbf{u}_L(k+n|k) \in \mathbb{U}_L$, $\mathbf{e}_{F_i}(k+n|k) \in E_{F_i} \ominus \mathcal{B}_{F_i}^n$, $\mathbf{e}_L(k+n|k) \in E_L \ominus \mathcal{B}_L^n$, $\mathbf{e}_{F_i}(k+N|k) \in E_{F_i}^f$ and $\mathbf{e}_L(k+N|k) \in E_L^f$.

Define the optimal cost at step k by $J_i^*(k)$, and the feasible cost by $\bar{J}_i(k+1)$, $i \in \mathcal{A}$, and following the approach presented in Marruedo et al. (2002), by employing Property-1 and Lemma-1, we can deduce that $\Delta J_L = \bar{J}_L(k+1) - J_L^*(k) \leq L_{J_L} \sum_{F_i \in \mathcal{N}_L} \Delta v_{i_{Max}} \delta_t - \|\mathbf{e}_L(k)\|^2$, $\Delta J_{F_i} = \bar{J}_{F_i}(k+1) - J_{F_i}^*(k) \leq L_{J_{F_i}}(\gamma + \rho + \kappa) - \|\mathbf{e}_{F_i}(k)\|^2$.

Considering the optimality of the solution, we conclude that $J_L^*(k+1) - J_L^*(k) \leq L_{J_L} \Delta v_{i_{Max}} \delta_t - ||\mathbf{e}_L(k)||^2$, $J_{F_i}^*(k+1) - J_{F_i}^*(k) \leq L_{J_{F_i}}(\gamma + \rho + \kappa) - ||\mathbf{e}_{F_i}(k)||^2$, which implies that the closed loop system is Input-to-State-Stable (ISS) Jiang and Wang (2001). This implies that the optimal costs are monotonically decreasing which consequently implies that the norm of the errors $\|\mathbf{e}_L(k)\|$, $\|\mathbf{e}_{F_i}(k)\|$ converge to a neighborhood of the origin, as $k \to \infty$.

5. RESULTS

In order to validate the algorithm in an application scenario, formation navigation with a time varying velocity, with 2 and 5 followers, were tested.

All simulations ran on an Intel Core-i7 8750H CPU, with 16GB of RAM available, performed in a Matlab environment. The Nonlinear MPC was implemented in ACADO, particularly Houska et al. (2011).

The desired relative positions are set as $\hat{\chi}_{F_1L} = [0 \ -1 \ 0]^T \ [m]$, $\hat{\chi}_{F_2L} = [0 \ 1 \ 0]^T \ [m]$. The desired attitude of the agents is kept constant and aligned with the inertial frame throughout the experiment, and therefore $\hat{\chi}_{LF_i}$, for $i = 1, 2$, is implicitly defined for this test. For the second test, three followers are added to the formation, with desired relative positions $\hat{\chi}_{F_3L} = [0.65 \ -0.65 \ 0]^T \ [m]$, $\hat{\chi}_{F_4L} = [0.65 \ 0.65 \ 0]^T \ [m]$, $\hat{\chi}_{F_5L} = [1 \ 0 \ 0]^T \ [m]$.

The first test shows the tracking capabilities of the proposed framework when a time-varying velocity is defined. This makes it possible to extend the framework to more complex scenarios. For this test, the desired formation velocity $\hat{\mathbf{v}}_F$ is set as

$$\hat{\mathbf{v}}_F(k|k+n) = \begin{bmatrix} 0.05 \\ 0.06\sin(0.5 \cdot \delta \cdot n + k) \\ 0 \end{bmatrix}, \forall n = 0 \ldots N-1 \tag{19}$$

leading to a sinusoidal trajectory as shown in Figure 2.

Figures 4 and 3 show the bearing error and velocity for each of the vehicles. Due to the time-varying trajectory, we observe that the agents achieve the equilibrium formation at $t = 10s$. For this test and for the followers, the desired velocity $\hat{\mathbf{v}}_F(k|k+n) = \hat{\mathbf{v}}_F(k)$, resulting in a bounded error for the predicted trajectory, as proved on Section 4. We also observe that the leader slowly accelerates to allow the formation to converge to the desired geometry at first, and then to track the desired formation velocity.

In this experiment, the average computational times were $4ms$ for the leader and $2.2ms$ for the follower. The maximum and minimum computational times are, respectively, $13ms$ and $3.5ms$ for the leader, and $7.3ms$ and $1.7ms$ for the followers. The settings for the NMPC are a receding horizon length of $N = 20$ and a sampling time $\delta = 0.05s$. Finally, the maximum velocity for the agents was set to $v_{i_{Max}} = 0.1$ [m/s].

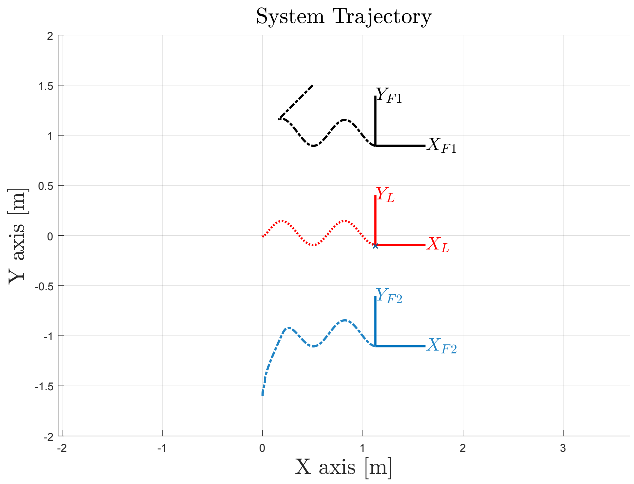

Fig. 2. Formation trajectory in the XY inertial plane.

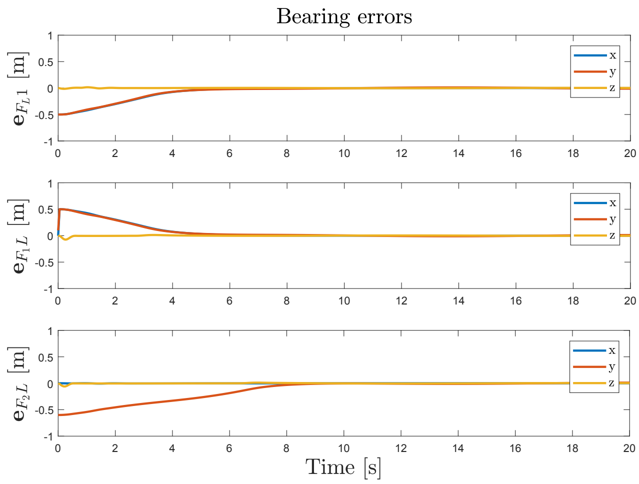

Fig. 3. Evolution of the bearing error through time, when the formation tracks a time-varying velocity.

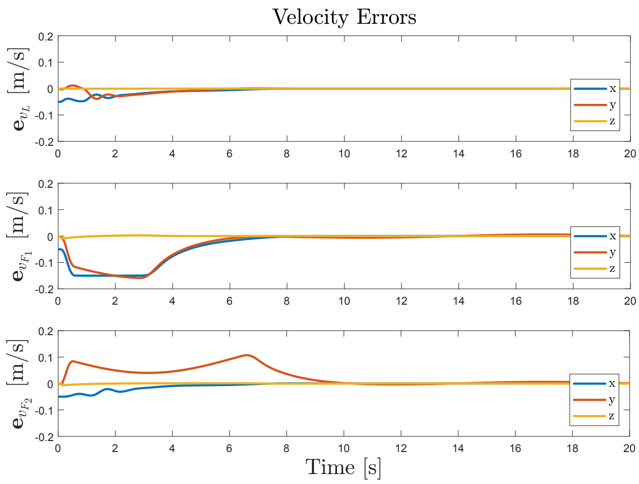

Fig. 4. Formation velocity error over time.

To better understand how the computational times are affected when followers are added to the formation, the second test was performed with 5 followers. For this test, we show the trajectory for the time-varying velocity, Figure 5, and the leader bearing and velocity error, on Figure 6.

For this test, the average computational time is $11ms$ for the leader, and $2.2ms$ for the followers. The maximum computa-

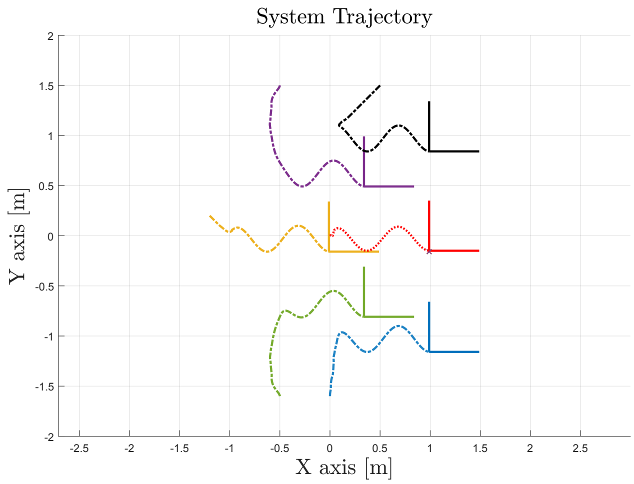

Fig. 5. Trajectory of the formation while tracking a time-varying velocity.

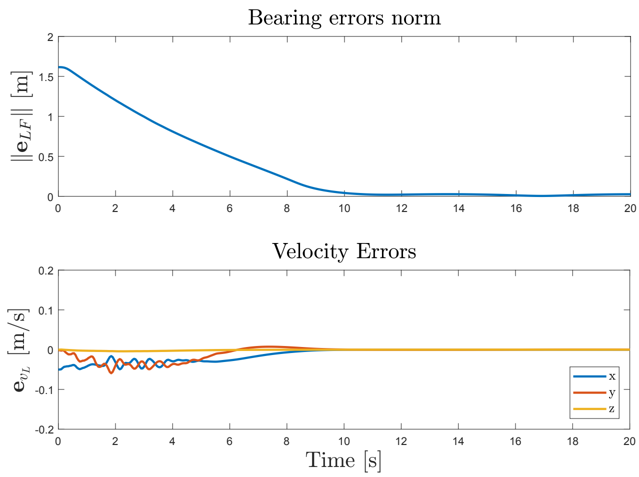

Fig. 6. Leader bearing error norm and velocity error.

tional times are $21ms$ and $4ms$, while the minimum are $9ms$ and $1.6ms$, for the leader and followers, respectively. Although the leader's computational time increase (although not proportionally) with the number of followers, we observe that the followers controller computational time remains the same.

6. CONCLUSION AND FUTURE WORK

In this work we presented a novel decentralized nonlinear model predictive control framework, with significant communication reduction and ensured stability properties. The approach is specially relevant for safety critical systems, where autonomy and resilience to failures is needed, as well as in scenarios where communication is costly, such as underwater robots. Moreover, these contributions also result in a fast controller, suitable to applications with agile systems. In the future, we plan to implement these methods on a experimental scenario, as well as extend the framework to allow other graph geometries, increasing the resilience of the system and better scale the leader controller to larger formations.

REFERENCES

Akhtar, A., Waslander, S.L., and Nielsen, C. (2012). Path following for a quadrotor using dynamic extension and inverse feedback linearization. In *2012 IEEE 51st IEEE Conference on Decision and Control (CDC)*, 3551–3556. IEEE.

Allgöwer, F., Findeisen, R., and Nagy, Z. (2004). Nonlinear model predictive control: From theory to application. *The Chinese Institute of Chemical Engineers*, 35(3), 299–315.

Bemporad, A. and Rocchi, C. (2011). Decentralized hybrid model predictive control of a formation of unmanned aerial vehicles. *IFAC Proceedings Volumes*, 44(1), 11900–11906.

Castillo, P., Dzul, A., and Lozano, R. (2004). Real-time stabilization and tracking of a four-rotor mini rotorcraft. *IEEE Transactions on control systems technology*, 12(4), 510–516.

Chen, J., Sun, D., Yang, J., and Chen, H. (2010). Leader-follower formation control of multiple non-holonomic mobile robots incorporating a receding-horizon scheme. *The International Journal of Robotics Research*, 29(6), 727–747.

Das, A., Subbarao, K., and Lewis, F. (2009). Dynamic inversion with zero-dynamics stabilisation for quadrotor control. *IET control theory & applications*, 3(3), 303–314.

Frazzoli, E., Dehleh, M., and Feron, E. (2000). Trajectory tracking control design for autonomous helicopters using a backstepping algorithm. In *Proceedings of the American control conference*, volume 6, 4102–4107.

Gandolfo, D.C., Salinas, L.R., Brandão, A., and Toibero, J.M. (2016). Stable path-following control for a quadrotor helicopter considering energy consumption. *IEEE Transactions on Control Systems Technology*, 25(4), 1423–1430.

Heshmati-Alamdari, S., Karras, G.C., Marantos, P., and Kyriakopoulos, K.J. (2019). A robust predictive control approach for underwater robotic vehicles. *IEEE Transactions on Control Systems Technology*, 1–12.

Houska, B., Ferreau, H., and Diehl, M. (2011). ACADO Toolkit – An Open Source Framework for Automatic Control and Dynamic Optimization. *Optimal Control Applications and Methods*, 32(3), 298–312.

Jiang, Z.P. and Wang, Y. (2001). Input-to-state stability for discrete-time nonlinear systems. *Automatica*, 37(6), 857–869.

Lee, T., Leok, M., and McClamroch, N.H. (2010). Geometric tracking control of a quadrotor uav on se(3). In *49th IEEE Conference on Decision and Control (CDC)*, 5420–5425. doi:10.1109/CDC.2010.5717652.

Mahony, R., Kumar, V., and Corke, P. (2012). Multirotor aerial vehicles: Modeling, estimation, and control of quadrotor. *IEEE Robotics Automation Magazine*, 19(3), 20–32. doi:10.1109/MRA.2012.2206474.

Marruedo, D.L., Alamo, T., and Camacho, E.F. (2002). Input-to-state stable mpc for constrained discrete-time nonlinear systems with bounded additive uncertainties. In *Proceedings of the 41st IEEE Conference on Decision and Control, 2002.*, volume 4, 4619–4624 vol.4. doi:10.1109/CDC.2002.1185106.

Rucco, A., Aguiar, A.P., Fontes, F.A.C.C., Lobo Pereira, F., and Borges de Sousa, J. (2015). *A Model Predictive Control-Based Architecture for Cooperative Path-Following of Multiple Unmanned Aerial Vehicles*, 141–160. Springer International Publishing, Cham.

Tayebi, A. and McGilvray, S. (2006). Attitude stabilization of a vtol quadrotor aircraft. *IEEE Transactions on control systems technology*, 14(3), 562–571.

Tsourdos, A., White, B., and Shanmugavel, M. (2010). *Cooperative path planning of unmanned aerial vehicles*, volume 32. John Wiley & Sons.